

Stability of viscous shock waves and beyond

Kevin Zumbrun

Department of Mathematics
Indiana University

Sponsored by NSF Grants no. DMS-0300487 and DMS-0801745

Short course, IHP: Lecture 15b



- Conclusion, entropy and stability.
- Toward viscous Majda's theorem.
- Further analogies between periodic and asymptotically-constant coefficient problems.
- Discussion and open problems.



V. Viscous analysis: Designer systems

An ingenious construction of S. Bianchini realizes any symmetric eigensystem. Consider the system

$$\begin{aligned}u_t + (A(v)u)_x &= (B(v)u_x)_x, \\v_t + \left(\frac{1}{2}u \cdot A'(v)u + \frac{1}{2}v^2\right)_x &= v_{xx},\end{aligned}\tag{1}$$

where $v \in R^1$. This contains a trivial standing viscous shock solution $(\bar{u}, \bar{v}) = (0, \bar{v}(x))$, where $\bar{v}(x) := -\tanh(x/2)$ is a shock of Burgers equation $v_t + (v^2/2)_x = v_{xx}$.

It has also the convex entropy $\eta(u, v) := \frac{1}{2}|u|^2 + \frac{1}{2}|v|^2$.



The rotating model

Linearizing (1) about the shock yields a decoupled linearized Burgers equation and

$$u_t + (A(\bar{v}(x))u)_x = (B(\bar{v}(x))u_x)_x, \quad (2)$$

essentially arbitrary. A natural choice is the *rotating model*

$$A(v) = R_{\theta(v)}A_mR_{-\theta(v)}, \quad B(v) \equiv \text{Id}, \quad (3)$$

where $R_\theta := \begin{pmatrix} \cos \theta & -\sin \theta \\ \sin \theta & \cos \theta \end{pmatrix}$, $A_m = \begin{pmatrix} 1 & 0 \\ 0 & -1 \end{pmatrix}$, and

$$\theta(v) = M\pi v \quad (4)$$

M an arbitrary real number, considering the family of stationary shocks $\bar{v}_\gamma(x) := -\gamma \tanh(\gamma x/2)$.

These are Lax 2-shocks, with a Lopatinski determinant $-2\gamma(\cos^2(M\pi\gamma) - \sin^2(M\pi\gamma))$ that changes sign infinitely often as γ increases from the small-amplitude limit $\gamma = 0$.



Numerical demonstration

Intuition: By [Z-Serre1999], we have $D(0) \sim \gamma\delta$, where γ is a stability index for the traveling-wave ODE and δ is the Lopatinski determinant. For γ small (slow-varying), the traveling-wave flow (hence γ) “tracks” rotations, for $\gamma \gg 1$ it does not. Hence, adjusting M and γ , we may tune the number and proximity of crossing roots to get Hopf (small target!!!).

Demonstration ($\epsilon =$ shock strength):

movie.mp4



Numerical justification/methods

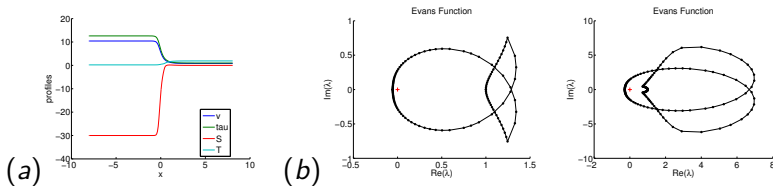


Figure: Viscous study results for $\bar{e}(S, \tau) = e^{S/\tau} + C^2 e^{C^{-1}(C^{-1}S - \tau)}$ with $S_- = -30$, $C = 10$, $\mu = \kappa = 1$, $(\tau_0, S_0) = (1, 0)$. (a) Viscous profile. (b) Integrated Evans function computed with the adjoint polar coordinate method, evaluated on a semi-circle with radius $R = 1$. Winding number is 1. (c) As in (b) but with $R = 250$.



Numerical methods (continued)

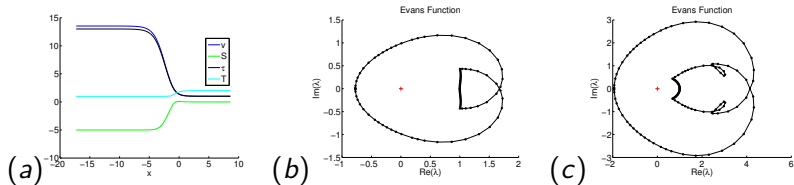


Figure: Viscous study results for $\bar{e}(S, \tau) = e^S/\tau + S + \tau^2/2$, $S_- = -5$, $\mu = \kappa = 1$, $(\tau_0, S_0) = (1, 0)$. (a) Viscous profile. (b) Integrated Evans function computed with the adjoint polar coordinate method, evaluated on a semi-circle with radius $R = 1$. Winding number is 1. (c) As in (b) but with $R = 250$.



Numerical methods (continued)

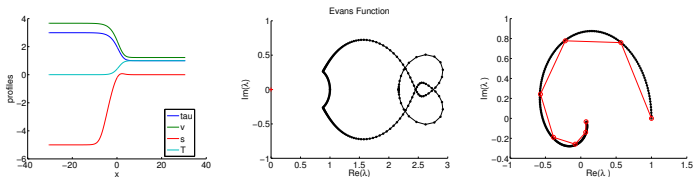


Figure: Viscous study results for $\bar{e}(S, \tau) = e^S/\tau + \tau^2/2$ with $(\tau_0, S_0) = (1, 0)$, and $S_- = -5$. (a) Viscous profile. (b) Integrated Evans function computed with the adjoint polar coordinate method, evaluated on a semi-circle with radius $R = 250$. Winding number is 1. (c) The Evans function evaluated at 8 points along a semi-circle of radius $R = 256$ is plotted with open circles. The best curve fit of the Evans function with $C_1 e^{C_2 \sqrt{\lambda}}$ is plotted with closed dots. The relative error between the two is 0.069.



Numerical methods (continued)

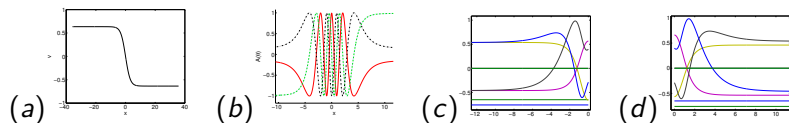


Figure: Rotating model with $M = 2.7174$, $\gamma = 0.635$. (a) Plot of profile $\bar{v}_\gamma(x) = -\gamma \tanh(\gamma x/2)$ against x . (b) Zoomed in plot of components of $A(\theta(x))$ against x . (c)-(d) Zoomed in plot of components of the evolved manifolds in the Evans function computations for $\lambda = 27/2$.



Conclusions

- Validates the inviscid theory of Erpenbeck-Majda (computations needed, not automatic).
- Resolves question brought up > 50 years ago by C. Gardner.
- Sheds new light on work of R. Smith and others on uniqueness.
- Possibility of Hopf bifurcation/galloping is a very interesting open question (MHD?).
- Coincidence or non-coincidence in interesting physical situations of viscous/inviscid stability remains open!

Remark: Leger-Vasseur *relative entropy condition* (relative entropy increasing along Hugoniot) *does* imply inviscid stability of extremal shocks! The “right” condition, generalizing ideas by Weyl, Bethe, Lax, ... a huge advance. (See [Texier-Z] for direct verification of Lopatinski).



VI. Toward viscous Majda's theorem: isentropic gas

(Inviscid result shown by Majda in 1 and multi-D for nonisentropic case.) Rescale

$(x, t, \tau, u, a_0) \rightarrow (-\varepsilon s(x - st), \varepsilon s^2 t, \tau/\varepsilon, -u/(\varepsilon s), a_0 \varepsilon^{-\gamma-1} s^{-2})$,
with ε so that $0 < \tau_+ < \tau_- = 1$, get

$$\begin{aligned}\tau_t + v_x - u_x &= 0, \\ u_t + u_x + (a\tau^{-\gamma})_x &= \left(\frac{u_x}{\tau}\right)_x,\end{aligned}\tag{5}$$

where $a = -\frac{\tau_+ - 1}{\tau_+^{-\gamma} - 1} = \tau_+^\gamma \frac{1 - \tau_+}{1 - \tau_+^\gamma} \rightarrow 0$ as $\tau_+ \rightarrow 0$.

High-Mach \sim pressureless gas limit...



Winding number computation

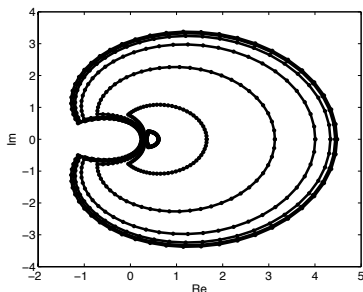


Figure: Convergence to the limiting Evans function as $\nu_+ \rightarrow 0$ for a monatomic gas, $\gamma = 5/3$. The contours depicted, going from inner to outer, are images of the semicircle under D for $\nu_+ = 1e-1, 1e-2, 1e-3, 1e-4, 1e-5, 1e-6$. The outermost contour is the image under D^0 , which is nearly indistinguishable from the image for $\nu_+ = 1e-6$.



The large amplitude limit

Theorem (HLZ)

For λ in any compact subset of $\Re\lambda \geq 0$, $D(\lambda)$ converges uniformly to $D^0(\lambda)$ as $v_+ \rightarrow 0$.

Proof.

Careful boundary layer analysis/asymptotic ODE estimates [HLZ,PZ]. □

Lemma (HLZ)

The limiting function D^0 is nonzero on $\Re\lambda \geq 0$.

Proof.

Energy estimate adapted from that [MN], small-amplitude result. □



Large-amplitude result

Corollary

For any $\gamma \geq 1$, isentropic Navier–Stokes shocks are stable in the strong shock limit, i.e., for v_+ sufficiently small.

- In practice, appears $v_+ \lesssim 10^{-4}$... Not determined so far analytically.
- Small-amplitude estimate like that of [Matsumura-Nishihara86] shows stability for $v_+ \gtrsim 0.4$ (\sim Mach 1.2)



Evans computation with interval arithmetic

(with Barker)

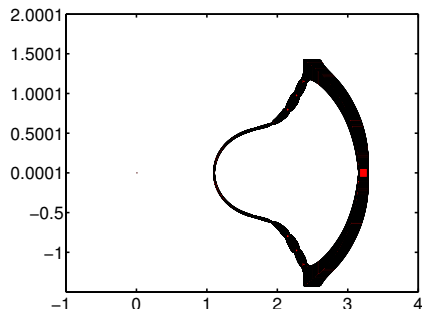


Figure: Evans contour with confidence intervals, $v_+ = 0.05$ (\approx Mach 10).
Computed down to $v_+ = 10^{-4}$ with similar results.



Rigorous Evans computations with interval arithmetic, similar to Barker's results for periodic waves. (However, different strategy based on conjugation rather than exponential convergence of analytic interpolation. Reason: "wrapping" phenomenon encountered in solution of ODE.) Here, error in approximation of limiting eigenvectors at $\pm\infty$ is mocked up conservatively as $\sim 10^{-3}$. Last (purely linear algebraic) step is to compute this error rigorously- in progress.



Extensions to full gas and multi-D

- Full gas in fact permits simplification due to absence of singularity in strong shock limit ($e_+ \rightarrow 0$ rather than $v_+ \rightarrow 0$.) This balanced against larger size of system (factor $\binom{5}{2} = 10$ vs. 3, at n^3 complexity roughly 30 times more effort- doable. Continuous orthogonalization should do better.
- Multi-D in principle do-able (good numerical results), but substantially more complexity. For the future...

Next wave: A 21'st century treatment of hydrodynamic stability, not possible before computational advance. (And perhaps more and more general computations as well.)



Coda: a result of Matsumura and Wang.

Ideal gas law $p = ae^{S/c_v} v^{-\gamma} = \Gamma T v^{-1}$, where S and T are thermodynamical entropy and temperature. Isentropic approximation: $p(v) = av^{-\gamma}$, $T = \Gamma v^{1-\gamma}$. Thus, temperature-dependent viscosity modeled by

$$\mu = \mu_0 T^\beta = \mu_0 v^{-\beta(\gamma-1)}, \quad \beta \geq 1/2. \quad (6)$$

Theorem (Matsumura–Wang2010)

For isentropic gas dynamics with density-dependence (6), all viscous shock profiles are spectrally (hence nonlinearly) stable.

Proof.

Energy estimate similar to that of [Matsumura–Nishihara85] (original small-amplitude result). Variable viscosity better! □



Comment

Like Leger-Vasseur result, a surprisingly strong “direct” result by other means (and may yet be others...)!



VII. Further analogies between periodic and asymptotically constant case

We have noted the analogy between conjugation lemma (of which we made crucial use!) for asymptotically constant coefficient and Floquet's lemma for periodic coefficient systems.

Going in the other direction, we have imported techniques from asymptotically constant problems to the nonlinear stability analysis of periodic waves and defect patterns.

Pursuing the analogy further, we derive (with Rodrigues) a Kawashima-type resolvent/damping estimate for periodic wave trains of St. Venant equations, crucial for treatment of large-amplitude waves (quite new).



Equations in co-moving coordinates:

$$\begin{aligned}\tau_t - c\tau_x - u_x &= 0, \\ u_t - cu_x + ((2F^2)^{-1}\tau^{-2})_x &= 1 - \tau u^2 + \nu(\tau^{-2}u_x)_x,\end{aligned}\tag{7}$$

Traveling-wave ODE:

$$-c\bar{\tau}_x - \bar{u}_x = 0, \quad \bar{u}_t - c\bar{u}_x + ((2F^2)^{-1}\bar{\tau}^{-2})_x = 1 - \bar{\tau}\bar{u}^2 + \nu(\bar{\tau}^{-2}\bar{u}_x)_x.\tag{8}$$

Key fact:

$$f(\bar{\tau})\bar{u}_x = cf(\bar{\tau})\bar{\tau}_x,\tag{9}$$

perfect derivative, so mean zero.



The slope condition

Linearized equations:

$$\begin{aligned}\tau_t - c\tau_x - u_x &= 0, \\ u_t - cu_x - (\alpha)\tau)_x &= \nu(\bar{\tau}^{-2}u_x)_x - \bar{u}^2\tau - 2\bar{u}\bar{\tau}u,\end{aligned}\tag{10}$$

where

$$\alpha := \bar{\tau}^{-3}(F^{-2} + 2\nu\bar{u}_x).\tag{11}$$

Slope condition of [Johnson-Z-Noble10] is $\bar{\tau}^3\alpha > 0$, yields symmetrizability. By (9), this holds on average, even if not pointwise...



Damping estimate

Define now the energy

$$\mathcal{E}(U) := \int \left(\frac{1}{2} \phi_1(x) \tau_x^2 + \frac{1}{2} \phi_2(x) \bar{\tau}^3 u_x^2 + \phi_3(x) \tau u_x \right). \quad (12)$$

A brief computation yields

$$\begin{aligned} \frac{d}{dt} \mathcal{E}(U(t)) &= \int \left(- \left(\frac{c}{2} (\phi_1)_x + \alpha \phi_3 \right) \tau_x^2 - \left(\frac{\nu}{\bar{\tau}^2} \phi_2 \right) u_{xx}^2 \right. \\ &\quad \left. + (\phi_1 - \alpha \phi_2 + \frac{\nu}{\bar{\tau}^2} \phi_3) \tau_x u_{xx} \right) \\ &\quad + O(\|u\|_{H^2} + \|\tau\|_{H^1})(\|u\|_{H^1} + \|\tau\|_{L^2}). \end{aligned} \quad (13)$$



Damping estimate cont'd

Taking (exponential weight as in shock case)

$$\frac{c}{2}(\phi_1)_x + \left(\frac{\alpha \bar{\tau}^2}{\nu} - \frac{\langle \alpha \bar{\tau}^2 \rangle}{\nu} \right) \phi_1 = 0, \quad (14)$$

$$\phi_1 - \alpha \phi_2 + \frac{\nu}{\bar{\tau}^2} \phi_3 = 0, \quad (15)$$

and

$$0 < \phi_1, \quad 0 < \phi_2 \equiv \text{constant} \ll 1, \quad (16)$$

we obtain after another brief computation

$$\begin{aligned} \frac{d}{dt} \mathcal{E}(U(t)) &= \int \left(- \left[\frac{\langle \bar{\tau}^2 \alpha \rangle}{\nu} \phi_1 - \frac{\alpha^2 \bar{\tau}^2}{\nu} \phi_2 \right] \tau_x^2 - \left(\frac{\nu}{\bar{\tau}^2} \phi_2 \right) u_{xx}^2 \right) \\ &\quad + O(\|u\|_{H^2} + \|\tau\|_{H^1})(\|u\|_{H^1} + \|\tau\|_{L^2}) \\ &\leq -\eta_1 (\|u_{xx}\|_{L^2}^2 + \|\tau_x\|_{L^2}^2) \\ &\quad + C_1 (\|u\|_{H^2} + \|\tau\|_{H^1})(\|u\|_{H^1} + \|\tau\|_{L^2}), \end{aligned} \quad (17)$$



Concluding argument

By Sobolev embedding and the fact that $\mathcal{E}(U) \sim (\|u_x\|_{L^2}^2 + |\tau_x|_{L^2}^2)$ modulo $\|\tau\|_{L^2}^2$, we obtain finally

$$\frac{d}{dt}\mathcal{E}(U(t)) \leq -\eta\mathcal{E}(U(t)) + C\|U(t)\|_{L^2}^2, \quad (18)$$

a standard *linear damping estimate*.

Remark: In the last step $\mathcal{E}(U) \sim (\|u_{xx}\|_{L^2}^2 + |\tau_x|_{L^2}^2)$, we have used in a critical way that $\int \left(\frac{\alpha\bar{\tau}^2}{\nu} - \frac{\langle \alpha\bar{\tau}^2 \rangle}{\nu} \right)$, hence ϕ_1 , remains bounded, a consequence of periodicity plus zero mean.

For shocks may substitute $\frac{c}{2}(\phi_1)_x + \left(\frac{\alpha\bar{\tau}^2}{\nu} - I\left(\frac{\alpha\bar{\tau}^2}{\nu}\right) \right)\phi_1 = 0$, where $I\left(\frac{\alpha\bar{\tau}^2}{\nu}\right)$ interpolates smoothly between $\frac{\alpha\bar{\tau}^2}{\nu}|_{x=\pm\infty}$, and obtain the same result (by exponential decay in place of mean zero).



Small viscosity (high frequency) limit

We have not discussed in these lectures the small-viscosity limit $\epsilon \rightarrow 0$ for

$$u_t + f(u)_x = \epsilon(B(u)u_x)_x,$$

treated by pseudodifferential/Kreiss symmetrizer methods in [Métivier-Z, Guès-M-Williams-Z] for shock and noncharacteristic boundary layers.

Perhaps the key point is to eliminate $1/\epsilon$ gradients in multi-scale (weakly nonlinear optics) by conjugating “fast variables” symbolically to constant coefficient, using the conjugation lemma, then apply symmetrizer methods like those in the inviscid case.

An interesting direction under investigation (with Métivier) is to treat similarly the small viscosity limit for periodic modulation, using Floquet’s lemma to conjugate to constant coefficients and applying symmetrizer estimates as in the shock case.



VIII. Discussion and open problems.

OPEN PROBLEMS.

- Numerical proof.
- Discrete and kinetic shocks, temperature-dependent transport. (Note important work of Liu, Yu and collaborators on Boltzmann equation.)
- Nonlinear stability of dispersive periodic waves.

Larger questions.

- Viscosity, entropy, and stability– Hopf bifurcation?
- Multi-dimensional flow with general geometry.*

